Kaikōura Earthquake Short-Term Project

Title: Assessment of existing concrete buildings in Wellington with precast floors

Leader: Professor Ken Elwood
Organisation: University of Auckland
Total funding (GST ex): $160,000

Assessment of existing concrete buildings in Wellington with precast floors

S.R. Corney, K. J. Elwood & R. S. Henry
Department of Civil and Environmental Engineering, University of Auckland

D.K. Nims
Department of Civil and Environmental Engineering, University of Toledo

ABSTRACT

The Kaikoura Earthquake resulted in extensive damage to precast concrete floor systems in multi-storey buildings in Wellington. Some of the observed damage states, mostly notably those induced in precast concrete hollow-core floors, were inconsistent with the damage observed during past research and led to uncertainties in the residual gravity load carrying capacity of the floor and the behaviour of the floor in future seismic events. A series of tests have been performed to address some of these uncertainties with this testing focusing on hollow-core floors containing transverse cracks. A total of four hollow-core floor specimens were prepared, the detailing of which was varied to encompass construction practices either consistent with typical 1980s construction or construction from this time period considered to represent the worst case. Each hollow-core specimen was tested in three stages: 1) damage consistent with observed damage is induced, 2) gravitational load consistent with reoccupation is applied and 3) seismic loading is applied to the damaged specimen. This sequence gives insight into the residual capacity of the floor, the vulnerabilities of various damage states and those damage states that should be addressed during retrofit. The results of the test programme are discussed along with the factors likely to induce non-ductile modes of hollow-core floors. The results of the project have directly informed the development of guidance for the seismic assessment of hollow-core floors incorporated in a proposed update to the NZ Seismic Assessment Guidelines currently under review by MBIE.

Introduction

The use of precast concrete floor units that incorporate a thin insitu topping is a common construction technique in New Zealand. Previous earthquake observations and research has shown that early use of precast concrete floors in ductile concrete frame structures had support connections that were in some cases inadequate to accommodate earthquake deformation (Iverson and Hawkins 1994; Matthews 2004; Fenwick et al. 2010; Corney et al. 2014). This inadequate detailing potentially results in the floor being susceptible to collapse at relatively low levels of structural drift. Of particular concern is the fact that there was a general lack of specific design requirements provided for the connections of precast concrete flooring systems during the 1980s, a time when the installation of such systems was extremely common. Hollow-core precast concrete floors were the predominant form of precast concrete floor construction during this time period (Park 2002; Brunsdon et al. 2017) and a large amount of research was subsequently performed on

this floor type. This research led to the development of improved support connection detailing capable of accommodating large earthquake demands for hollow-core floors in new structures (Standards New Zealand 2006) as well as the development and installation of retrofitting techniques within a large number of existing buildings. A targeted damage assessment programme identified significant damage to precast concrete floors in Wellington buildings following the 2016 Kaikoura earthquake (Kestrel Group 2017). In many cases, the observed damage was inconsistent with the failure modes of hollow-core precast concrete floors identified during previous research, bringing into question the understanding of the failure modes, the residual capacity of the floor once this damage had been sustained and the effectiveness of the existing retrofitting techniques (Henry et al. 2017). To address these concerns, an experimental programme has been performed to investigate the behaviour of hollow-core precast concrete floors containing damage consistent with the observed damage states under further loading. Of particular importance is the additional loading required to cause floors with the observed damage states to lose reliable load paths to the support connection.

Previously identified failure modes of hollow-core floors

Large scale floor tests at the University of Canterbury (UC) highlighted two actions that were found to cause the most damage to the precast concrete floor unit support connections. These are illustrated in Figure 1. First, as a multi-story building deforms when subjected to lateral earthquake loading, the support beams rotate relative to the floors which remain approximately horizontal. This relative rotation between the precast concrete floor unit and its support causes forces to be developed in the continuity reinforcement placed in the insitu topping (Fenwick et al. 2010). Second, in ductile frames, the plastic hinges that form in the beams elongate during cyclic loading as a result of inelastic straining of the beam reinforcement and dislodgment of aggregate at tensile crack locations that cause these cracks to not fully close during load reversal. The frame dilation due to this axial elongation in the beams oriented parallel to the precast concrete floor units results in the distance between floor supports increasing and a consequent reduction in the floor unit seating. Additionally, the supporting ledge can spall due to the prying action applied by the floor unit (Jensen 2006).

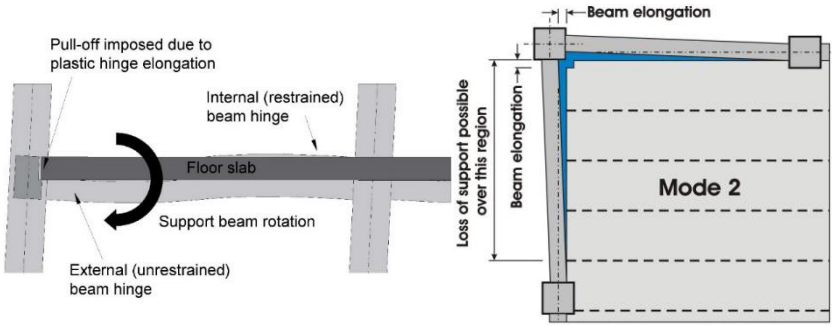

a) Support beam rotation relative to horizontal floor

b) Beam elongation induced cracking

Figure 1. Floor support connection actions resulting from frame drift (after Mathews (2004))

Hollow-core units in New Zealand are generally produced using high strength concrete and dry-cast extrusion systems. Production requires that there is only longitudinal prestressing with no transverse reinforcement, resulting in a potentially brittle unit. When damage is induced in a floor diaphragm which contains potentially brittle precast units, it is desirable for the deformation to be concentrated at the unit-to-beam interface where the seating ledge is able to provide adequate vertical support to the floor and damage to the unit is avoided. This is in contrast to the typical 1980s design practice that the precast units should be embedded into the support to prevent movement of the unit relative to the support beam. Fenwick et al. (2010) summarises a number of potential undesirable failure modes of hollow-core units that were observed during testing. These are primarily a result of support beam rotation and parallel beam elongation. Three of the key failure modes of hollow-core floor units are illustrated in Figure 2 and consist of:

- **Loss of support:** The unit loses seating due to a combination of insufficient length of support to accommodate earthquake deformations, spalling of the support beam ledge, and entrapment of the end of the precast unit. Following loss of seating, the vertical reaction force to support the unit is transferred to the insitu topping concrete which will likely cause the topping to peel off the unit and a subsequent collapse of the floor unit.
- **Positive moment failure:** If the strength at the back face of the unit is sufficient to result in a weak section forming away from the support ledge. Cracking in this location will generally be initiated at low drift levels with any additional deformation becoming concentrated at this weak section. As the crack width at this location increases, gravity load transfer is compromised resulting in collapse of the floor unit.
- **Negative moment failure:** Where the continuity reinforcement is terminated too close to the support, the drop in negative moment capacity can result in a weak section. A crack in the top of the unit at this location can propagate into the webs of the unit causing loss of gravity load carrying capacity and collapse of the floor unit.

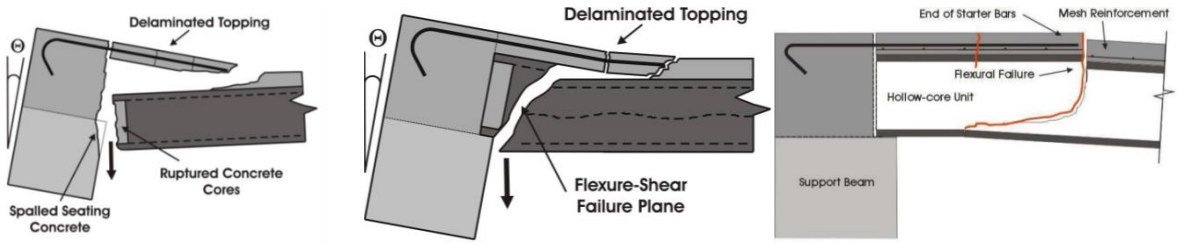

a) Loss of support failure (Jensen 2006) b) Positive moment failure (Jensen 2006) c) Negative moment failure (Woods 2008)

Figure 2. Previously identified failure modes for hollow-core floors

Damage to precast concrete floors during the 2016 Kaikoura earthquake

An initial review of Wellington buildings following the 2016 Kaikoura earthquake indicated that, while some of the observed damage to precast concrete hollow-core floors was consistent with that observed during the past research, several new damage patterns were identified in several buildings.

Therefore, new questions have arisen regarding the safety of precast concrete floor units with earthquake-induced cracks (Brunsdon et al. 2017; Henry et al. 2017).

Observed damage included transverse cracking and web cracking. Transverse cracking close to the supports of hollow-core units was also observed during the 2010/2011 Canterbury earthquake sequence (Corney et al. 2014), but was more prevalent in the Kaikoura earthquake due to the prevalence of 1980s hollow-core construction in Wellington and the earthquake's characteristics.

a) Close to the support

b) ~300 mm out from the support

Figure 3. Transverse cracking of hollow-core units

Figure 3a shows an example of transverse cracking within 100 mm of the beam support. This type of cracking was consistent with the previously identified failure modes shown in Figure 2. The bottom flange prestressing strand is not well developed at the ends of the unit and may also be affected by strand draw-in or slip. As a result, transverse cracks near the support can significantly impact the shear capacity near the ends of the hollow-core floor units. Several buildings were also found where single transverse cracks in the hollow-core units occurred at approximately 300 mm from the support as shown in Figure 3b. The location of the crack on the top surface typically corresponded to the end of the starter bars and, in many cases, the crack was found to extend vertically through the full depth of the unit. While past research has shown that negative moments at supports may lead to cracking at the end of the starter bars (see Figure 2c), this cracking was previously found to extend into a diagonal crack in the unit's web in contrast to this observed vertical crack. Given the distance of the transverse crack from the support (typically 300 mm), the bond for the bottom flange prestress strand is likely sufficient to sustain gravity loads, but further widening of the crack in aftershocks was a concern. Note that typical retrofits of hollow-core floor systems in New Zealand only provide support for units within approximately 100 mm of the supporting beam and would not prevent collapse of units failing at vertical cracks at approximately 300 mm from the support. It was therefore identified that further research is needed to understand the cause of this cracking pattern, the capacity in future aftershocks, and potential retrofit techniques to address this failure mode.

Experimental investigation

A series of tests have been performed to investigate the residual capacity of hollow-core floors containing transverse cracks as observed in a number of Wellington buildings and described above. The testing was designed to ascertain the varying behaviour of hollow-core floors containing cracks

that have formed either at the base of unit or in the topping at varying distances away from the support connection. A total of four test specimens (labelled HC1-HC4) were prepared and the support connection detailing of each of these specimens are summarised in Table 1. After damage was induced in the specimen consistent with a targeted damage state, the hollow-core floor was subjected to gravitational and seismic loading to investigate the residual capacity of the floor. The detailing of all test specimens emulates construction either consistent with typical 1980s construction or construction from this time period considered to be worst case. In general, it was intended that the connection detailing and applied loading combinations were representative of those that would likely be encountered in a typical office structure containing 12 m spanning 300 mm deep precast concrete hollow-core floor (300HC) units. 300HC units were selected on the basis that they are the deepest units (and therefore the most vulnerable to damage) common in existing structures to provide a suitable benchmark for the seismic performance of hollow-core floors containing such damage.

Pull-off deformations were not applied to the support connections of all specimens. The test specimens that were subjected to pull-off deformations were considered to be located adjacent to the parallel perimeter frame beam where the most extensive damage due to this deformation would be induced (see Figure 1b) while the test specimens where only rotational seismic deformations were applied to the connection were intended to represent a hollow-core unit located at a sufficient distance from the perimeter beam that elongation of the beam did not affect the support connection. In general, pull-off deformation was not applied to the specimens that only contained cold-drawn (665) mesh at the support connection due to the supposition that floors containing this detailing would fail at low levels of drift.

Table 1. Testing specimen detailing summary

Test	Continuity reinforcement		Core fill
	Type	Extension	
HC1	665 mesh	-	300 mm
HC2	665 mesh	-	75 mm plug
HC3	D12 at 300	600 mm	300 mm
HC4	D12 at 300	600 mm	75 mm plug

Specimen design and construction

The specimens were designed in accordance with common New Zealand construction practices and a diagram of the specimen detailing is shown in Figure 4. Standard 300HC units with a specified compressive strength of 45 MPa were used. The specimens were cut to a length of 4000 mm such that they contained a sufficiently long length of floor for the actions at the support connection to be simulated. The units were seated directly on top of a 50 mm wide unreinforced support beam ledge (with a concrete compressive strength of 45 MPa) and temporarily propped at the other end prior to testing.

The continuity reinforcement and core fill was varied between the four specimens to encompass the variability in 1980s construction. The differences in detailing consisted of the extent of the hollow-core voids that insitu topping concrete was permitted to flow into and the use or omission of

continuity reinforcement. Where continuity reinforcement was placed at the support connection, the continuity reinforcement detailing was consistent for each test as described below and the mesh that was placed in the insitu topping was terminated at the end of the hollow-core unit. Where continuity reinforcement was omitted from the support connection, the mesh was extended to cross the unit-to-beam interface. The main features of the connection design included:

- 50 mm unit seating on top of an unreinforced beam ledge.
- A 75 mm thick insitu topping concrete with a specified compressive strength of 30 MPa. The 75 mm thick topping was selected on the basis that the precamber in the precast units would typically result in a topping thickness of approximately this depth at the support connection despite 65 mm thick toppings generally being specified.
- Four (D12) deformed bars of 12 mm diameter, with a characteristic yield strength of 300 MPa (Grade 300), extended 600 mm into the topping concrete at 300 mm spacings as continuity reinforcement. The D12 continuity reinforcement was lapped onto 665 cold-drawn mesh placed in the 75 mm topping over the entire length of the floor.
- Voids either blocked with dam plugs, allowing approximately 75 mm of concrete to flow into the voids, or with cardboard approximately 300 mm from the end of the unit. The different core fill variations were selected on the basis of the proximity to the support connection of the intended damage state.

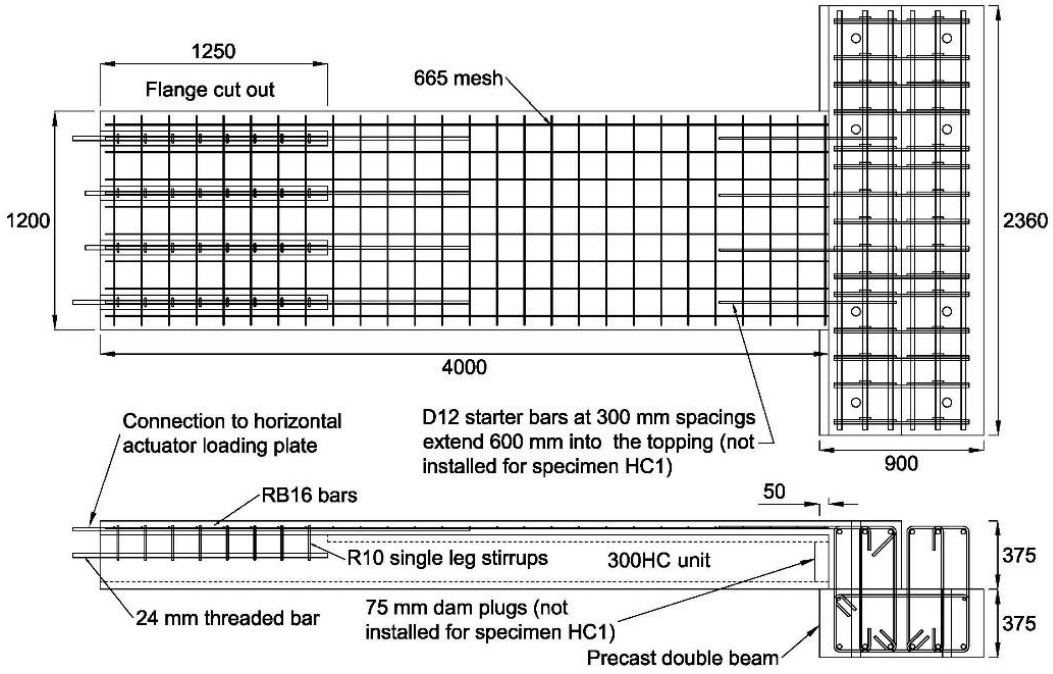

Figure 4. Specimen design (shown for HC4)

Test setup

A sub-assembly test setup was used that was similar to that developed during the previous UC research (MacPherson 2005; Jensen 2006) with the test setup consisting of a floor unit-to-beam connection over the width of a single 1200 mm wide precast unit and the seismic deformations simulated by displacement applied at the far end of the specimen. The testing was performed within a structural testing laboratory which enabled the use of a strong floor and strong wall to apply loads

to the specimen. As indicated in Figure 4 a precast double beam was manufactured as part of the specimen construction so as to allow for a stable base block post-tensioned to the laboratory strong floor that allowed for deformations to be applied to the support connection. Two hydraulic actuators were used to apply displacements to the far end of the specimen. Figure 5 is diagram of the sub-assembly test setup. The 4000 mm long hollow-core unit was seated on the support beam at one end and supported by the vertical actuator that was positioned 400 mm in from the other end of the unit. The testing of specimens was designed to be carried out in three stages:

Stage 1: Inducing damage:

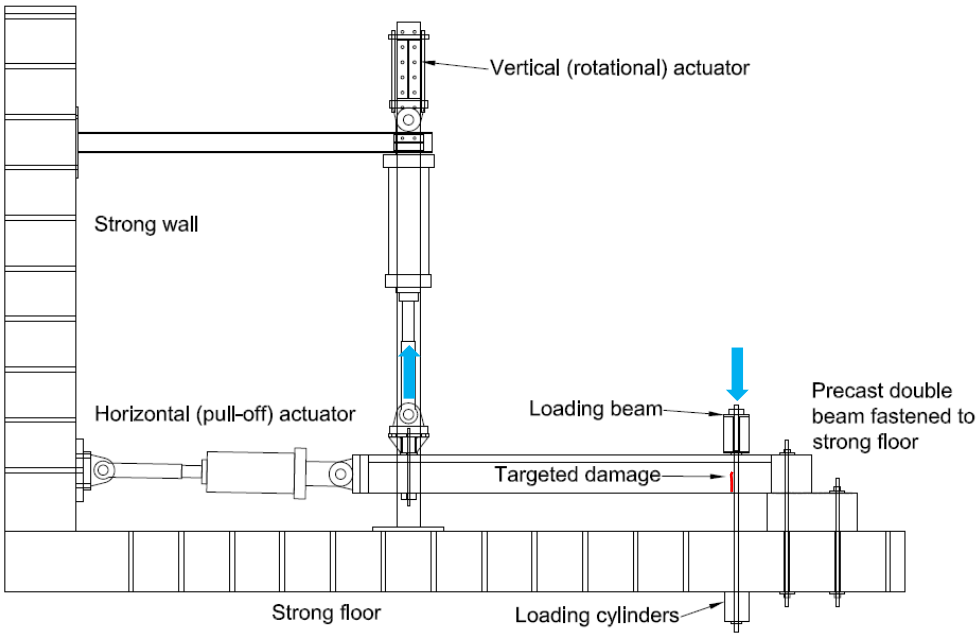

a) Inducing positive moment crack

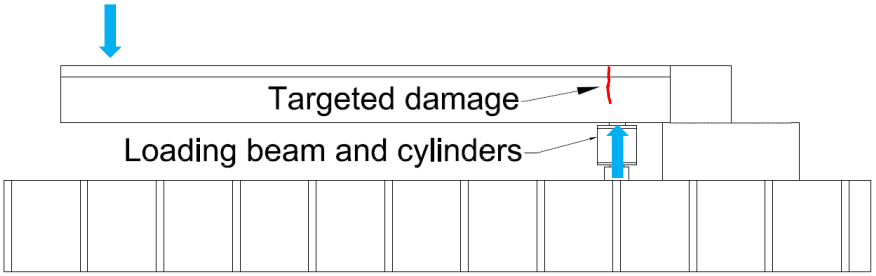

b) Inducing negative moment crack

Figure 5. Test setup (for stage 1)

During the first stage, damage was to be induced within the specimen consistent with a target damage state. It was intended that to achieve a crack at the base of the unit at the desired location; the end of the unit adjacent to the support connection would be held rigidly while the vertical actuator rotated the floor either upwards. The loading beam that held the unit down was fastened in place by hydraulic cylinders that acted against the strong floor as indicated in Figure 5a. Figure 5b shows how the test setup was altered in order to induce a crack in the topping. It was intended that loading would be applied so as to induce a thin crack of approximately 0.2 mm width through

approximately half the height of floor, consistent with floor damage that would result in the floor potentially being considered reoccupiable.

Stage 2: Residual gravity load capacity:

During the second stage of testing vertical loading was applied to the damaged floor to test residual gravity load carrying capacity of the floor. As the floor was considered to be potentially reoccupiable, loading was applied that generated a support connection reaction consistent with that due to the '1.2G, 1.5Q', permanent and imposed gravitational load case from the New Zealand Structural Design Actions Standard (Standards New Zealand 2002), uniformly distributed over the surface of the floor of the typical structure. For this load case, an additional gravitational load of 110 kN was applied at a distance of 1300 mm from the support connection (3.5 times the depth of the floor) to induce a reaction force of 89 kN. The distance at which the vertical load was applied away from the support was dictated by the minimum distance so as to ensure any enhancement of the capacity of the floor section for any particular crack was prevented as well as by the location of holes in the strong floor. This vertical load was applied through the loading beam, pulled down by cylinders loading against the strong floor similar to during the first stage of testing and as indicated in Figure 6a.

a) Full gravity loading setup

b) Seismic gravity loading setup (with loading beam clear of specimen)

Figure 6. Test setup photos

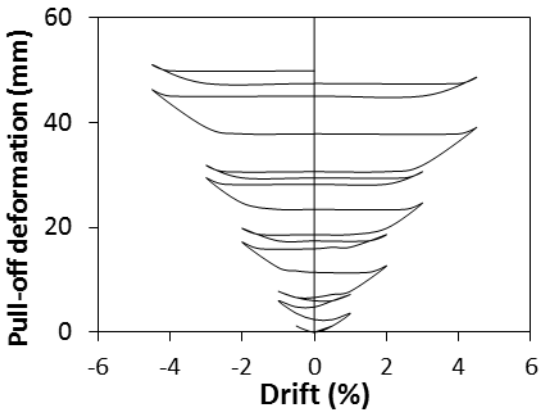

Figure 7. Seismic loading protocol

Stage 3: Residual seismic loading capacity:

During the third stage of testing, the connection was subjected to simulated seismic loading to progressively increasing magnitudes of deformation until failure of the specimen. Due to the anticipated vulnerability of the support connections to non-ductile failure modes, a large number of cycles were not applied to the connection to gauge the performance of the floor. A loading protocol was established such that a single cycle would be applied to ±0.5% drift followed by two cycles to ±1.0% drift, ±2.0% drift, ±3.0% drift and ±4.5% drift or until failure of the specimen. Rotational deformations were achieved by lifting the end of the hollow-core unit using the vertical actuator. The applied rotation was (conservatively) considered to be equivalent to the drift of the structure. During the tests in which elongation was applied, pull-off displacements were achieved using the horizontal actuator to provide a tension force in the unit (see Figure 5). This simulates the growth of the parallel beams in the building due to the development of beam plastic hinges. The horizontal actuator was connected to reinforcement placed at the far end of the unit during specimen construction (see Figure 4). To accurately simulate both support beam rotation and parallel beam elongation at each drift step of the loading protocol, a relationship between rotation and elongation previously developed by Jensen (2006) was adapted to suit the test specimens. The deformations applied during the loading protocol are shown in Figure 7. Additional gravitational loading was also applied to the top of the hollow-core unit to simulate the loading likely to be present at the support connection as seismic deformations are applied. This is consistent with the gravitational loading component of the seismic design load case, 'G, ψE Q, Eu' (Standards New Zealand 2002). This load was applied by a steel billet frame with a weight of 72 kN that caused a support connection reaction force of 56 kN. Figure 6b shows the test specimen with the steel billet frame positioned on top of the floor.

Instrumentation

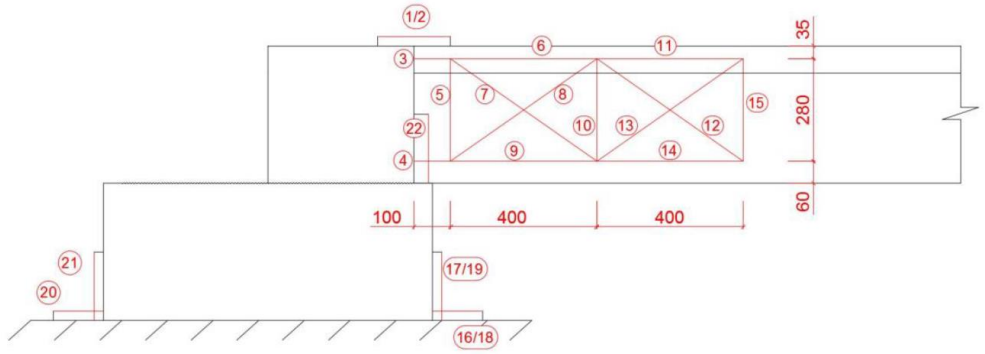

a) Gauges to measure deformation components within specimen (eastern side)

b) Gauges to measure vertical dislocation of floor

Figure 8. Location of displacement gauges within specimen

A series of gauges were used to measure the forces and deformation of the test specimen, including:

- Load cells installed on both actuators and the loading beam to measure the force applied.
- Displacement gauges installed on both actuators to determine the rotational and pull-off deformations applied to the support connection.
- Displacement gauges to measure deformation component in the hollow-core unit and topping as well as at the floor-to-beam interface. The locations of these gauges can be seen in Figure 8a. During several of the tests gauges in addition to those shown were also installed to monitor the opening of any induced cracks.
- Displacement gauges positioned along the floor to measure vertical displacements. These gauges are shown in Figure 8b.

Test specimen HC1 results

Induced damage

A crack formed at the top of the floor as a direct result of the setup process at a distance of 380 mm from the support beam. This distance is approximately the length to which the voids had been filled with insitu concrete during specimen construction. This crack is indicated by the red line shown in Figure 9 and it can be seen that the crack had initiated at the top of the floor and propagated vertically through the topping and approximately halfway through the 300HC unit. It was deemed that the test would be continued without inducing further damage such that the subsequent behaviour of the floor with this damage state could be determined. This damage was consistent with that observed in several Wellington buildings (Henry et al. 2017). Furthermore, this crack was also induced as a direct result of the support connection detailing.

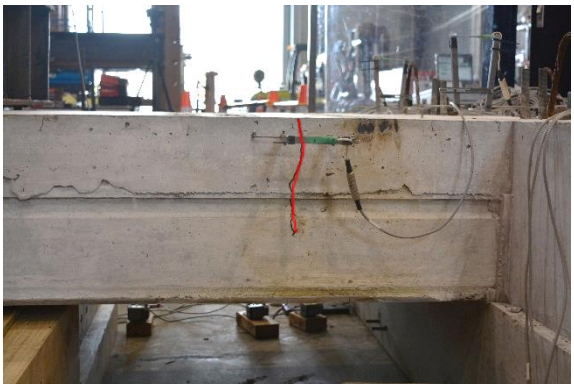

Figure 9. HC1 induced damage (indicated by red line)

Testing observations

Gravitational loading was subsequently applied to the support connection as Stage 2 of the test was carried out. The previously sustained damage resulted in the topping crack widening under the applied load and propagating 120 mm toward the support connection. The path of propagation of this crack is shown in Figure 10a, indicated by the line marked on the specimen. The fact that this crack propagated under gravitational loading alone prior to further seismic loading justifies concerns about the suitability for floors with such damage to be reoccupied.

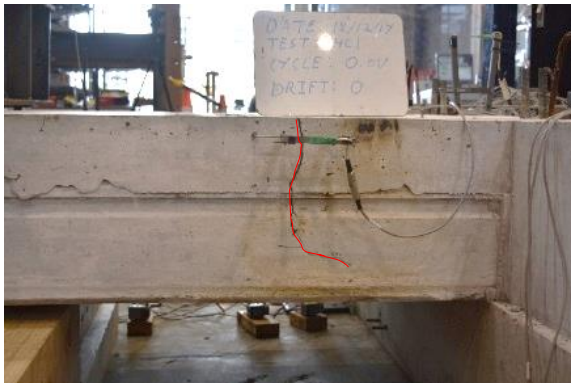

a) Gravitational loading

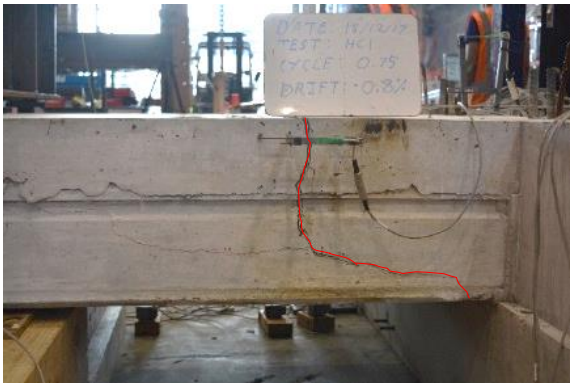

b) -0.9% drift

c) +1.0% drift

d) +2.0% drift

e) -2.0% drift

f) -1.5% drift (2nd cycle to -2.0%)

Figure 10. HC1 test progression photos (with red line indicating location of critical crack prior to becoming visible in photos)

The connection was then subjected to simulated seismic loading as Stage 3 of the test with only cyclic rotation applied during this test. The progression of damage to the support connection throughout seismic loading is shown in Figure 10b through to Figure 10f. Due to an issue with the vertical actuator, deformation to -0.9% was sustained by the connection during the first seismic loading cycle. This deformation led to the horizontal propagation of the crack above the bottom flange of the 300HC unit to within 100 mm of the support beam ledge as well as through the webs away from the support connection (see Figure 10b), resulting in a failure mechanism comparable to that shown in Figure 2c. The subsequent application of positive rotation led to this crack propagating

through the bottom flange at the base of the unit and approximately 60 mm out from the support beam ledge. Figure 10c shows the state of the floor once drift to +1.0% had been sustained. At this stage, the crack width at the soffit was approximately 4 mm (0.3 times the diameter of the prestressing strand) and the vertical dislocation of the floor was approximately 4 mm. The authors consider that both the crack width at the prestressing strands and the vertical dislocation were representative of a crack that no longer has reliable means to transfer shear forces. The positive rotational deformation applied to the connection was then increased +2.0%. It was deemed that subjecting the connection to this increased positive rotation would provide more insight to the behaviour of the floor; specifically, the widening of the critical crack at the unit soffit that would result in the prestressing strands being unable to transfer shear forces to the support connection. Figure 10d shows the state of the floor at +2.0% drift and it can be seen that the crack width at the unit soffit had increased to approximately 7 mm with vertical support for the floor being retained as a result of shear transfer provided by dowel action of the prestressing strands combined with that provided by the floor bearing on plugs of concrete within the filled cells spanning across the crack. This is an unreliable load transfer mechanism. It should be noted that the application of pull-off deformations would have likely resulted in collapse of the floor prior to this stage in the test. Further cycles were applied to ±2.0% with the floor becoming increasingly susceptible to collapse as the crack opened and less shear transfer could be provided by the floor bearing on the filled cores. The mesh remained intact across the cracked interface and rather an additional crack formed in the topping with the topping becoming delaminated from the unit as shown in Figure 10e. Ultimately, the width of the crack became sufficiently large and the collapse of the floor occurred at -1.5% during the second cycle to -2.0%, as shown in Figure 10f.

Measured response

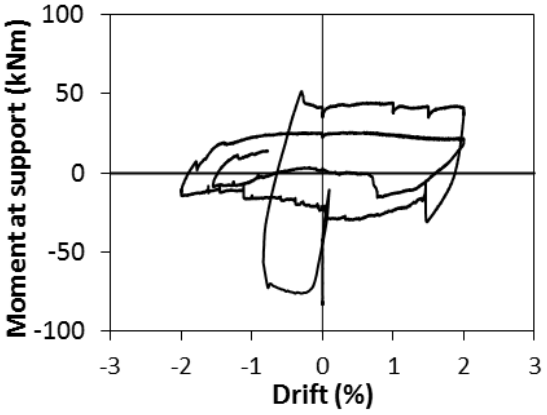

a) Response at support connection

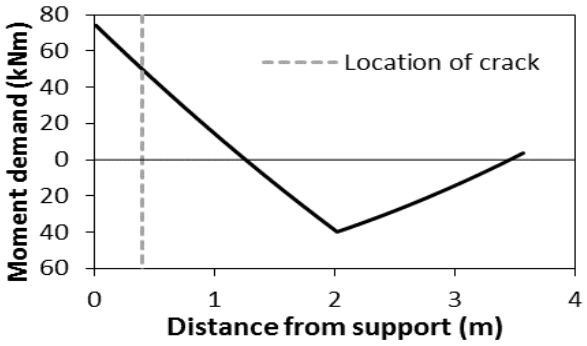

b) Moment demand at maximum negative moment

Figure 11. HC1 moment-rotation response

Figure 11a shows the moment at the support as the floor was rotated about the floor-to-beam connection during Stage 3 of the test. The moment at the support was determined from the combined loads applied by the self-weight of the floor, the weight of the billet and force in the vertical actuator. The response of test specimen HC1 indicates a partially fixed support prior to the application of any rotational deformation, shown by the negative moment at the support. The initial seismic loading cycle to -0.9% drift is characterised by a sharp peak in negative bending capacity that

is then degraded prior to the application of further negative loading cycles later in the test. The delamination of part of the topping during loading to -2.0% drift (see Figure 10e) and the extent of damage sustained by this point in the test would have prevented significant negative moments from being sustained at the cracked interface and rather the floor dropped considerably relative to the support as it was rotated downwards. Figure 11a also indicates that significant positive moment capacity was developed by the connection during the first cycle to +2.0% drift with the damage sustained by the connection causing this capacity to drop considerably during the second cycle to this level of rotation.

Figure 11b shows the moment demand along the floor as the maximum negative moment is induced at the support (during loading to -0.9% drift). The magnitude of the moment demand at the crack relative to the support is consistent with the fact that deformation became concentrated at this location during the test. The lightly reinforced topping results in the capacity at the crack being significantly less than that required to crack the floor at the unit-to-beam interface. The proximity of the crack to the support connection and the shear at the support are therefore key factors in determining the susceptibility of negative moment cracks to widen as relative rotation is induced at the support.

Vertical dislocation of the floor relative to the ground was measured by a displacement gauge positioned adjacent to the cracked interface (800 mm into the floor from the support beam) and began during the first loading cycle to -0.9% drift as indicated in Figure 12a. The skewed response of this dislocation is the result of the measurement recorded by this gauge being dependent on the rotation applied to the floor while the values measured at the zero drift cycles provide an accurate record of the dislocation of the floor relative to the beam at these points in the test. Following the first cycle to -0.9% drift, the residual dislocation of the floor was approximately 2 mm, a dislocation considered to be indicative of the floor vertical support being sustained by unreliable load paths. Following the first cycle to +2.0% and beginning at approximately +1.5% drift, the dislocation of the floor begins to rapidly increase due to the onset of the topping delamination discussed above (compare Figure 12a to the sharp drop in moment capacity at this point in the test shown in Figure 11a). The dislocation continually increases as the floor drops relative to the support as shown in the damage progression photos in Figure 10.

The measured crack widths throughout the progression of the test in the topping and the unit soffit are shown in Figure 12b and Figure 12c respectively. The crack width at the soffit approximates the length over which the prestressing strands are required to support the floor via dowel action. It can be seen in Figure 12c that this crack opened up approximately proportionally to the increase in positive rotation applied to the floor whilst remaining constant through the subsequent negative loading cycle. Measurements of the topping crack width became distorted during the latter testing cycles due to the vertical dislocation of the floor and partial delamination of the topping concrete. The residual crack widths at the zero drift position each cycle are a record of the elongation of the floor as the floor pries apart under cyclic loading.

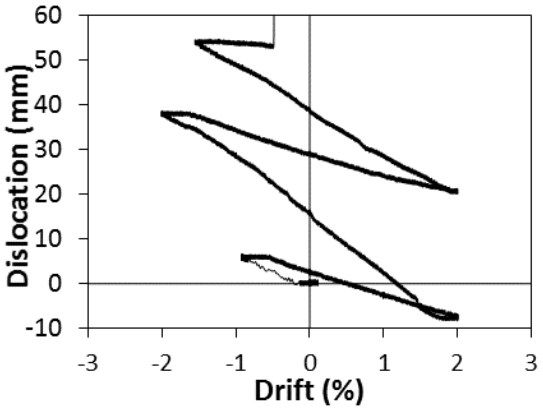

a) Floor vertical dislocation (gauge D2)

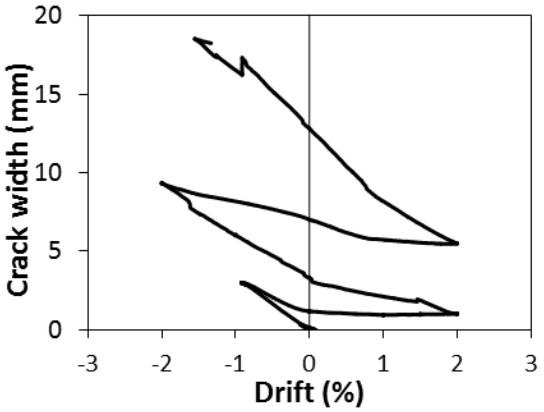

b) Topping crack width (additional gauge shown in Figure 10)

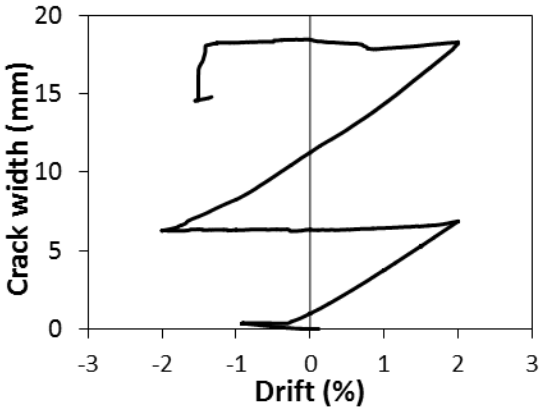

c) Soffit crack width (gauge 9)

Figure 12. HC1 measured deformations

Test specimen HC2 results

Induced damage

The intention for specimen HC2 was to induce a crack at the unit soffit approximately 300 mm from the support connection, similarly to those observed in some Wellington buildings (Brunsdon et al. 2017), and to investigate the subsequent behaviour of floors containing these cracks at a similar distance from the support. For this damage to be achieved, the setup shown in Figure 5a was established. However, in attempting to induce this damage it was found that the development of the prestressing strands at this section had been underestimated and the capacity required to crack the unit soffit was unable to be exceeded. Furthermore, the floor had cracked at the unit-to-beam interface during setup (see Figure 13a) thereby limiting the capacity of the connection to sustain positive moments. Figure 14 illustrates the bending profile of the floor and it can be seen that if the prestressing strands were close to full development, the gradient of the bending moment profile of the floor would need to be very sharp to generate sufficient demand at the targeted crack location to induce this soffit crack. For this sharp change in moment demand to be achieved, the loading beam was required to apply a load greatly in excess of the calculated floor shear capacity. For the

bending moment profile in the floor shown in Figure 14, a maximum of 490 kN was applied by the loading beam to induce a shear of 450 kN at the support. This induced shear was more than twice the calculated shear capacity of the floor, as calculated from the New Zealand Concrete Structures Standard (Standards New Zealand 2006). As a result of the magnitude of the applied loading, shear cracking was induced near the support as shown by the photos in Figure 13. However, a vertical crack did form at the unit soffit on the eastern side of the connection simultaneously with this shear crack (see Figure 13a), indicating the potential for the targeted crack damaged to be induced for assessment using this setup.

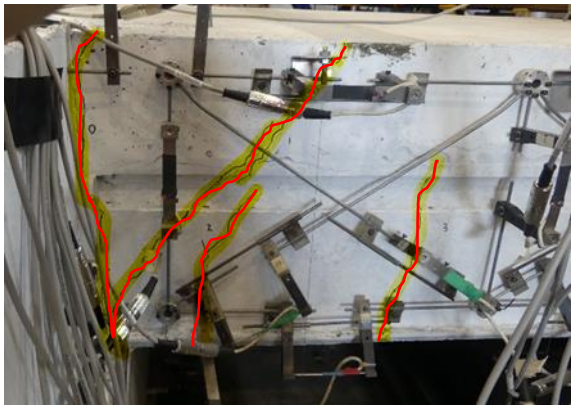

a) Eastern side

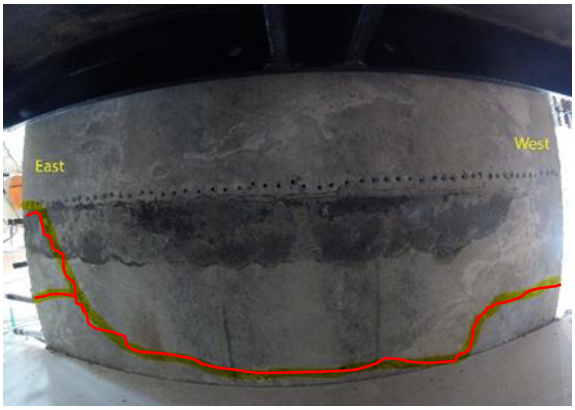

b) Underside

Figure 13. HC2 induced damage

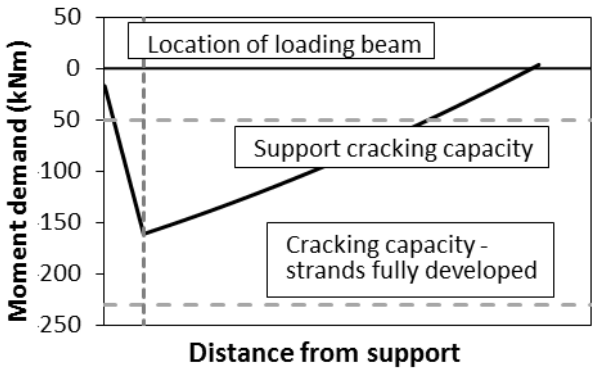

Figure 14. HC2 moment demand along floor at maximum applied positive moment

Testing observations

Although the floor had sustained damage not originally targeted for this test, the residual capacity of a floor where a positive moment crack has formed through the unit soffit near the edge of the support (see Figure 2b) could still be investigated. Residual gravity testing of the specimen resulted in no change in the state of damage within the floor. This lack of damage under the simulated gravitational actions was anticipated as significantly larger loads had previously been sustained by the floor while the damage was being induced in the specimen. Furthermore, the resulting shear crack propagated past the support ledge at some locations and so shear could still be transferred by the floor bearing on the support.

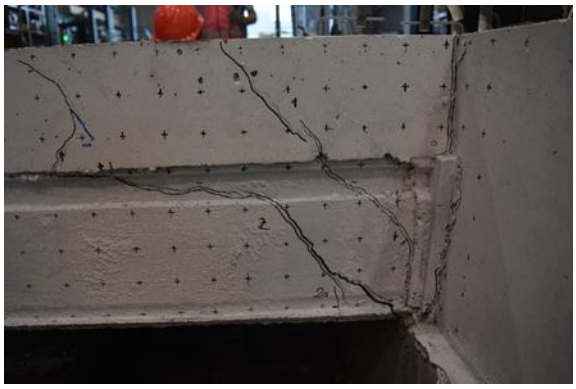

a) +1.0% drift (second cycle)

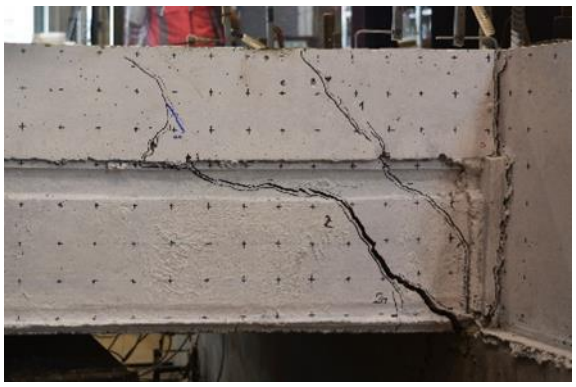

b) +2.0% drift

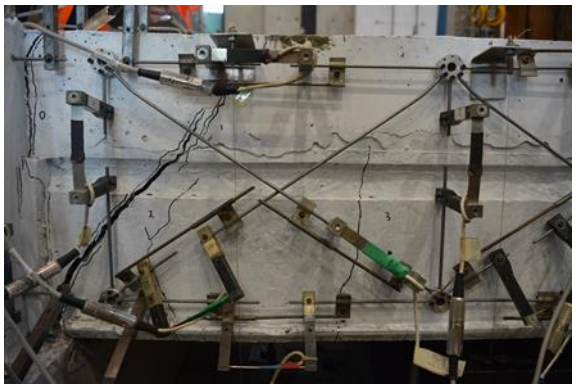

c) +2.0% drift – eastern side

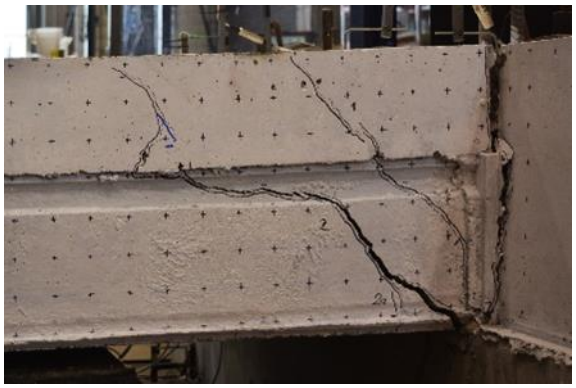

d) -2.0% drift

e) Collapse

f) Fractured webs

Figure 15. HC2 test progression photos

Seismic loading was subsequently applied to the connection and, similarly to the testing of specimen HC1, it was deemed that rotational deformation alone would be applied due to the expected susceptibility to failure at low levels of applied deformation for a floor with this connection detailing (cold-drawn mesh as continuity reinforcement) and the nature of the sustained damage. The progression of damage of the specimen through increasing cycles is shown in Figure 15. Positive rotations were accommodated by the growth of the diagonal crack at the unit soffit near the support ledge. This crack grew through successive cycles to 0.5%, 1.0% and 2.0% (see Figure 15) while the

crack 300 mm into the floor remained closed as anticipated due to the significant development of the prestressing strands at this location (see Figure 15c). Deformation during the negative loading cycles was concentrated in the topping at the floor-to-beam interface (see Figure 15d) with the top of the diagonal shear crack remaining closed. The mesh crossing the interface gradually fractured during successive cycles to -1.0% and the following cycle to -2.0% at crack widths ranging between 4 mm and 7 mm for these eight bars.

During the first cycle to +2.0% drift the width of the shear crack at the soffit resulted in sufficient dropping in the floor that the floor was deemed to have failed during this cycle with a maximum sustained drift of 1.0%. The width of the crack at this stage in the test was approximately half of the diameter of the prestressing strands. The maximum crack width that a floor is considered to be able to accommodate at this location is the equivalent to the strand diameter (with these units containing 12.9 mm strands). Following this point, the floor remained intact through loading to a second cycle to +2.0% and then a monotonic increase in positive loading with the floor ultimately collapsing at an applied drift of approximately 3.5% and a soffit crack width of approximately 1.5 strand diameters. It should be noted however that the bearing of the floor on the eastern side of the specimen (see Figure 15d) would have helped to enable support to be maintained to such a large deformation during this particular test. Furthermore, the application of pull-off deformations would have resulted in this critical crack width being sustained at a lower level of simulated drift. Figure 15f shows the state of the hollow-core unit with fractured webs following failure.

Measured response

Figure 16 shows the moment-rotation response of the floor throughout the progression of the applied loading. The degradation the connection due to the induced damage meant that no appreciable positive moment capacity was developed and capacity was limited by the resistance of the prestressing strands as they debonded from the concrete. This capacity decreased during the final monotonic cycle as the strands became free of the end of the unit. Capacity during the negative loading cycles was provided by the mesh bars at the interface in tension. This tensile force resulted in an ultimate negative moment capacity of 38 kNm prior to the fracture of these bars, characterised by the ratcheting response of the connection. The ultimate negative moment capacity of the floor away from the connection is approximately 54 kNm due to contribution of the partially developed prestressing strands. This capacity was measured during the testing of specimen HC1 and shown previously in Figure 11b. Furthermore, the demand away from the connection is also reduced as the floor section becomes closer to the point of contra-flexure. As a result of the relative demand-to-capacity ratios, negative rotational deformation can be expected to become concentrated at the floor-to-beam interface for a cracked section where the topping reinforcement is constant through the floor-to-beam interface.

This concentration of deformation at the interface is indicated in Figure 17 also. Figure 17b indicates that there was some elastic straining of the mesh crossing the diagonal shear crack during the cycles to -0.5% and -1.0% while the mesh was still intact at the floor-to-beam interface. These strains were reduced as the demand dropped following the fracture of the bars at the interface. This crack is indicated to open up during the latter positive cycles in the test, however, this is only as a result of the floor dropping.

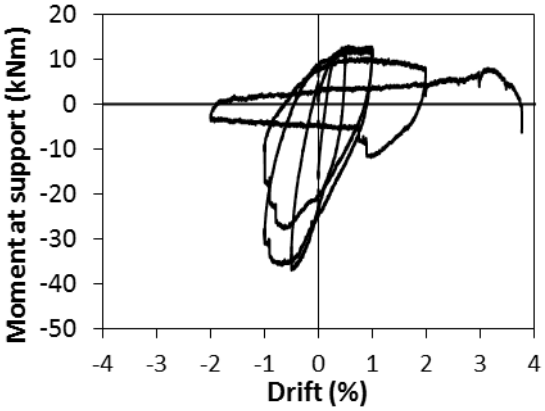

Figure 16. HC2 moment-rotation response

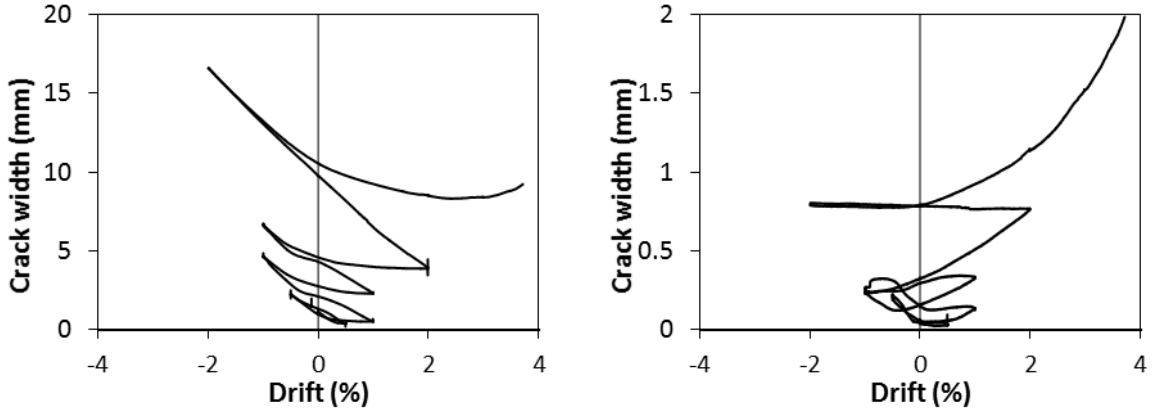

a) Interface crack (gauge 3)

b) Crack away from support (gauge 6)

Figure 17. HC2 measured deformations in the topping

Figure 18a shows the growth of the shear crack at the support ledge during the test. The vertical component of this crack as it widened (shown in Figure 18b) meant that the dislocation of the floor went beyond 2 mm during the first cycle to +2.0% drift as described above, by which point it can be considered that the floor had lost reliable load paths to the support. Figure 18b also indicates that the floor had dropped considerably prior to the strands properly being pulled out of the end of the unit and collapse of the floor. Despite the formation of two cracks further into the floor on the eastern side of the connection (see Figure 15c) these cracks did not open up significantly during the test as deformation became concentrated at the crack close to the support where the prestressing strands were the least developed. It can be seen in Figure 18c that these cracks had opened up slightly during the earlier cycles but no further deformation was concentrated here later in the test as the connection degraded and the strand slipped out of the end of the unit.

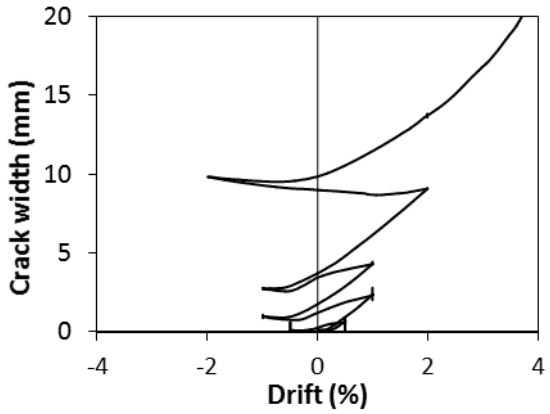

a) Soffit crack at support (gauge 4)

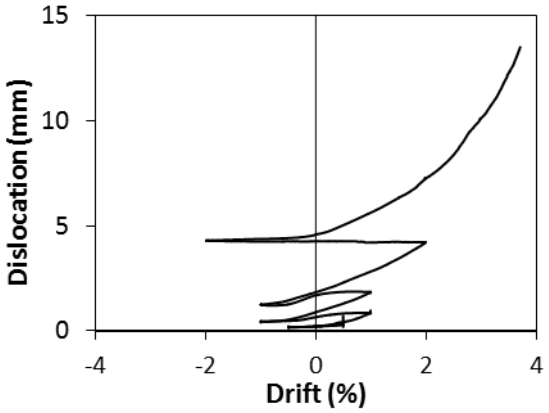

b) Vertical dislocation at support crack (gauge 5)

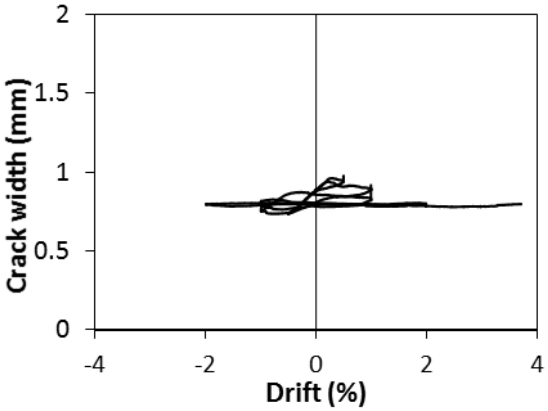

c) Topping crack at support (gauge 3)

Figure 18. HC2 measured deformations at the soffit.

Test specimen HC3 results

Induced damage

Due to the inability to induce a positive moment crack 300 mm away from the support during the testing of specimen HC2, specimen HC3 was altered to further help enable this targeted crack to form. The hollow-core soffit was cut to a depth of 20 mm at the intended crack location to reduce the cracking capacity and it was ensured during the setup of this specimen that the floor-to-beam interface remained uncracked. As a result of these factors, the difference in bending moment capacity of the two sections was reduced meaning that a lower shear force would be required to achieve the necessary bending moment profile in the floor. It was additionally considered that the shear capacity at the support would be greater due to the cores of this specimen being filled with concrete to a distance of 300 mm along the unit (see Table 1). However in attempting to induce this crack it was found that due to uneven bearing of the hollow-core unit on the support ledge, the shear capacity of this specimen was reduced in comparison to that of specimen HC2 and a diagonal crack was initiated on the western side of the connection, as shown in Figure 19. The moment able

to be induced at the critical section was only approximately the same as that induced within specimen HC2 and no crack was initiated despite the presence of the notch. It was concluded that it was unfeasible for the targeted crack to form in these particular units as the attempts made to induce it within the laboratory test setup imposed a significantly higher demand on the uncracked section than this section would be exposed to in a real building. Furthermore, the inability to induce this crack brings into question how cracks of this nature were enabled to form within a number of units in Wellington buildings as discussed earlier. It is considered that these cracks were likely the result of the stresses imposed on a newly cast unit or due to significant strand pull-in within the unit that would lower the cracking capacity.

Rather than investigate further the behaviour of a floor with a shear crack near the support ledge, it was decided that a negative moment crack would be induced at the end of the starter bars present within this specimen (see Table 1). The negative moment crack was induced using the setup illustrated in Figure 5b and is shown in Figure 19. The load require to bring about this negative moment crack was 84 kNm, slightly in excess of the estimated cracking capacity of 70 kNm. The nature of this crack was similar to that induced in specimen HC1 but it was located further from the support (approximately 670 mm from the support). Cracks at the end of the starter bar have been observed in some buildings (Brunsdon et al. 2017), induced due to a localised stress concentration at this location as loading is imposed either throughout the life of the structure or due to seismic deformation.

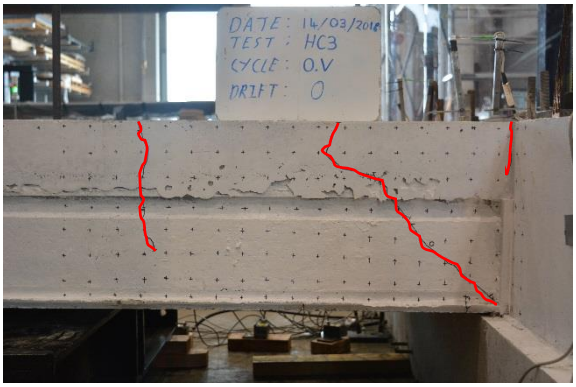

Figure 19. HC3 induced and gravity load damage

Testing observations

Gravitational loading was subsequently applied to the connection. The negative moment demand resulted in cracking in the topping at the floor-to-beam interface as shown in Figure 19 while significant deformation was not observed at the locations of the induced cracks. Simulated seismic loading was then applied to the connection with the billet positioned on the floor 1.55 m from the connection. The cycles to ±0.5% drift were simulated with rotational deformation alone applied to the connection while combined rotational and pull-off deformations were imposed throughout the remainder of the test, following the protocol shown in Figure 7. The progression of damage throughout the test is shown in Figure 20. All of the damage became concentrated at the crack at the end of the unit while the induced crack at the end of the starter bars remained closed (see Figure 20d). The shear crack on the western side of the specimen was monitored with a

displacement gauge and was also measured to remain closed, therefore not affecting the behaviour of the floor during the remainder of the test.

a) -1.0% drift

b) +2.0% drift

c) -2.0% drift

d) +2.0% drift (second cycle)

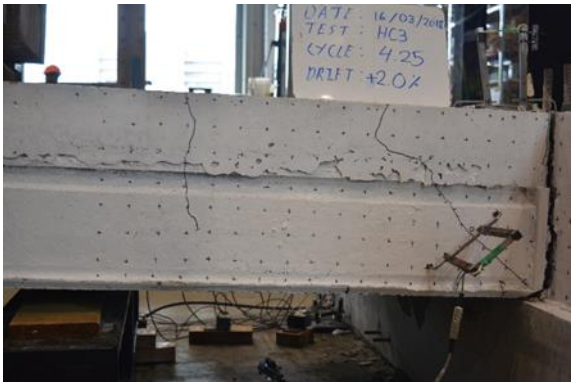

e) +2.0% (second cycle) – western side

Figure 20. HC3 test progression photos

As deformation was concentrated at the floor-to-beam interface, this became a test to investigate loss of support failure for the floor with a typical gravity load on the floor and subsequently Figure 20a - Figure 20d show the spalling of the support ledge and vertical dislocation of the floor. Spalling damage increased during the test resulting in a significant drop in the floor on the eastern side of the

connection during the first cycle to -2.0% drift (see Figure 20c) and the floor was deemed to have lost support at this point. During the subsequent cycles the floor slipped further relative to the support ledge on the eastern side of the connection while a lack of spalling on the western side of the support ledge meant that seating for the unit on top of the ledge was maintained (see Figure 20d) and a significant twist was induced in the unit. The instability of the specimen due to this twist resulted in the need to end the test following the completion of the second cycle to ±2.0% drift, at which point the floor had dropped 33 mm relative to the support beam on the eastern side, as measured by gauge D1 (see Figure 8b). Vertical support for the floor was provided by the kinking of the D12 starter bars which remained intact during these final cycles.

Measured response

Figure 21a shows the moment-rotation response of the connection. As axial tension was applied through the horizontal actuator to achieve the pull-off deformation targets during the cycles to ±1.0% onwards, the negative moment capacity of the connection was reduced following the first cycle to -0.5% drift where only rotation was applied. This reduction in negative moment capacity was despite the fact that the starter bars were strain hardening as the applied deformation was increased. As a result, the peak negative moment demands in the floor were induced while the stress in the starter bars was only approximately equivalent to their yield strength. For the deformation targets to be achieved during the positive loading cycles, the floor was in compression where axial load was applied. As a result of this compression force through the unit, it can be seen in Figure 21a that the positive moment capacity of the floor remained high despite cracking at the floor-to-beam interface and a drop in capacity during the rotation-only cycle to +0.5% drift.

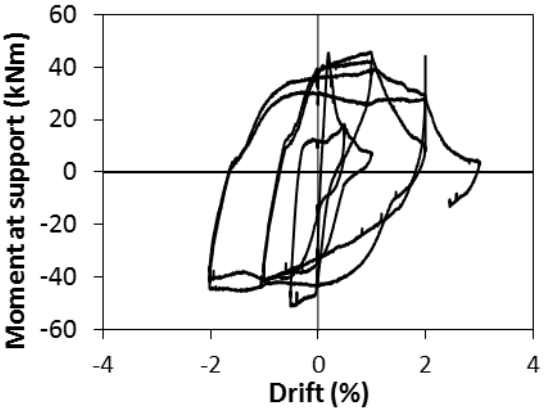

a) Response at support connection

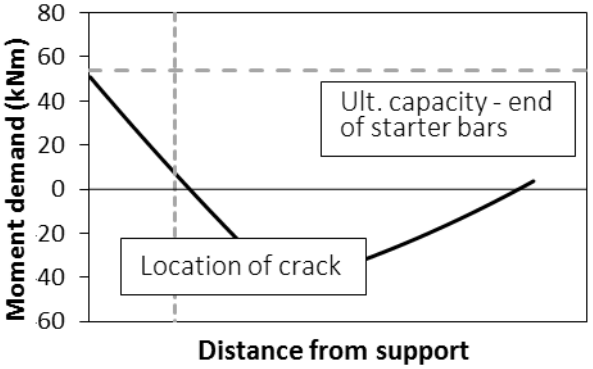

b) Moment demand at maximum negative moment

Figure 21. HC3 moment-rotation response

Figure 21b shows the bending moment profile along the floor at the point where the maximum bending moment demand was sustained at the connection. It can be seen from this bending moment profile that the demand was well below the capacity of the floor at the end of the starter bars and hence significant stress was not induced in the mesh. It should be noted that the location of the additional gravity load relative to the support was calculated based on inducing a reaction force at the support connection equivalent to that in the typical structure where the floor was simply supported. However, the increase in reaction force at the support connection with an increase in

negative moment demand was more significant for this short spanning specimen in comparison to that of an actual (longer spanning) floor and, as such, the reaction force at the support is overestimated. As a result of the larger reaction force, the bending moment gradient is steeper than it would be for the targeted typical structure and the demand at the end of the starter bars is reduced.

The calculated ultimate negative moment capacity of the floor at the end of the starter bars shown in Figure 21b was based upon an assumed level of stress in the prestressing strands as well as assumptions made by Woods (2008) regarding the strain present in the mesh. This capacity was calculated to be 54 kNm, approximately equivalent to that measured during the testing of specimen HC1.

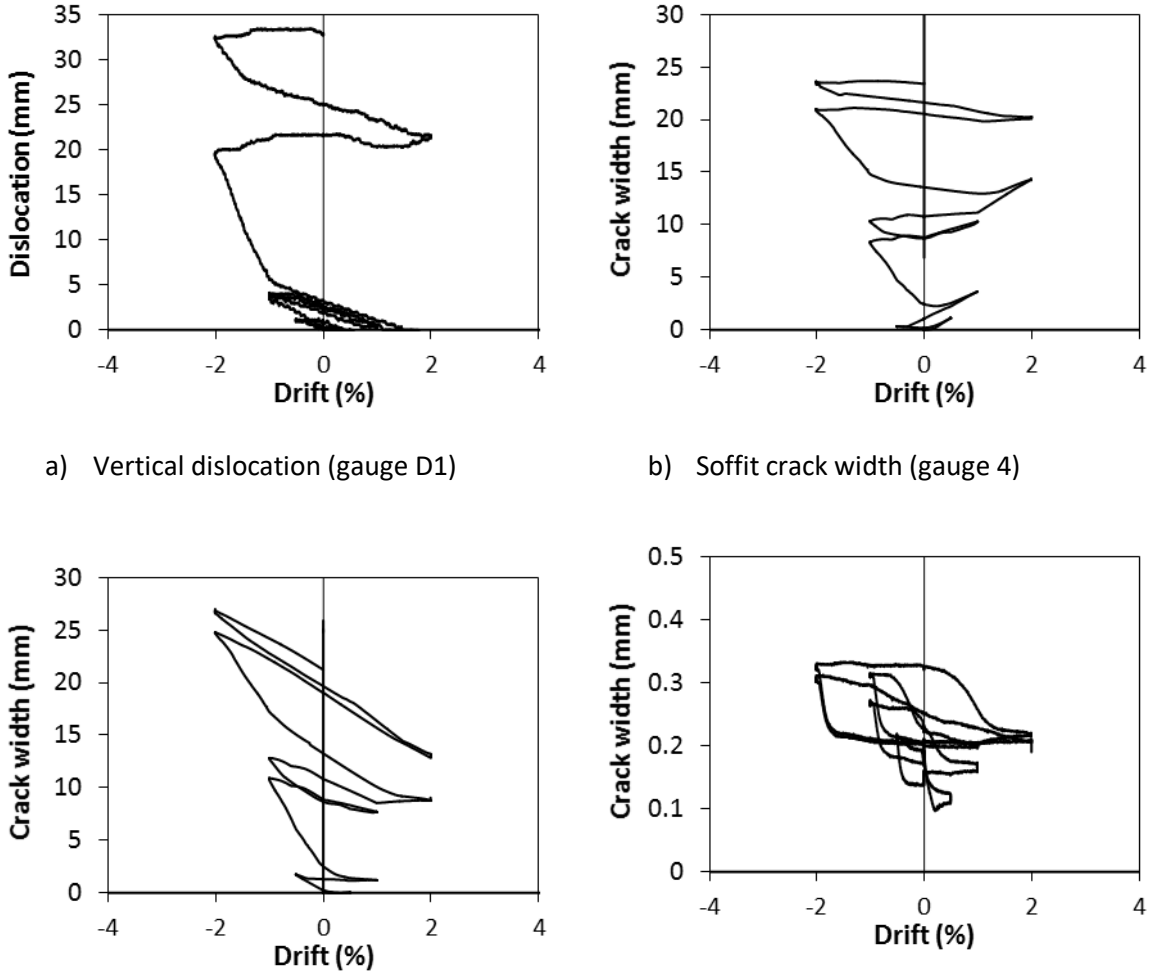

a) Vertical dislocation (gauge D1)

b) Soffit crack width (gauge 4)

c) Topping crack width (gauge 3)

d) Crack width at end of starter bars (gauge 11)

Figure 22. HC3 measured deformations

Figure 22 shows deformation measurements recorded throughout the seismic test. Unlike specimens HC1 and HC2, the crack widths sustained were induced as a direct result of the seismic loading protocol and the applied pull-off deformation; rather than the floor being pushed away from the support due to the applied rotation. Figure 22a shows the vertical dislocation of the floor recorded on the eastern side of the floor with the vertical dislocation on this side significant due to

the localised spalling shown in Figure 20 above. A minor drop in the floor was recorded during the first cycle to -1.0% followed by a major drop at approximately -1.0% during the first cycle to -2.0% drift, consistent with the observed damage and the considered point of failure.

The effective length of spalling was approximated from the applied deformation at the time the floor was considered to fail subtracted from the initial length of seating. As the initial seating for the unit was measured to be 47 mm and the applied deformation towards the height of the ledge was measured to be 14 mm at the point of failure (see Figure 22b); the effective length of spalling was approximated to be 33 mm, sustained following a maximum achieved drift of 2.0%.

Figure 22c and Figure 22d show the deformation within the topping at the floor-to-beam interface and at the end of the starter bars respectively. It can be seen that almost all of the applied deformation was concentrated at the floor-to-beam interface, consistent with the damage observations discussed above, while Figure 22d indicates that only small elastic strains had been sustained by the mesh during the negative loading cycles.

Test specimen HC4 results

Induced damage

Following the testing of specimen HC3 and the inability to induce a negative moment failure during this test, the intention for specimen HC4 was to successfully induce a negative failure within the floor such that the loading conditions required to induce this failure could be verified for floors containing various starter bar configurations. As for test specimen HC3, a crack was induced in the floor close to the location at which the starter bars were terminated. The load required to bring about this negative moment crack was 81 kNm, a similar load to that required to induce this crack during the testing of specimen HC3. In order to help induce the negative moment failure to occur at low levels of drift, full gravity loading was not applied during this test as it was considered that this would likely crack the topping at the floor-to-beam interface, while it was desired that deformation would not be concentrated there.

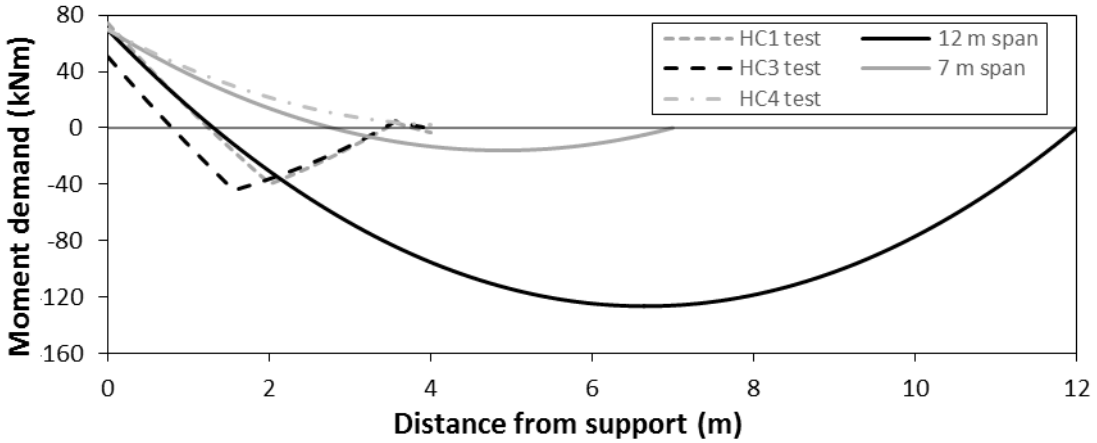

Figure 23. Significance of negative moment demands during tests

Seismic loading was applied to the support connection without the placement of the billet on the floor. The omission of the additional gravity load meant that a very low vertical reaction force was

induced at the support connection, resulting in a shallow bending moment gradient and therefore a higher bending moment demand at the end of the starter bars relative to that at the end of the unit. Figure 23 illustrates the significance of the bending moment demands induced along the floor for each of specimens HC1, HC3 and HC4 relative to the moment profile within the 12 m spanning floor of the typical structure. In the case of specimen HC4, the slope of the bending moment gradient results in the point of contra-flexure in the floor being close to the vertical actuator, located 3.55 m from the support, simulating a very low gravity load case for this shallow bending moment gradient, as indicated by the 7 m floor span shown in the diagram, unlikely to be constructed using 300HC units.

Testing observations

Figure 24 shows the state of the specimen throughout the progression of seismic loading. Similarly to specimen HC3, only rotation was applied to the specimen during the cycles to ±0.5% drift while it was intended that combined rotational and pull-off deformations would be applied to the support connection throughout the subsequent cycles. During this test however, the negative cycles were applied prior to the corresponding positive cycle, unlike the previous tests where the positive cycles were first applied. During the cycle to -0.5% drift, the applied rotation resulted in inelastic straining of the mesh and, consequently, widening of the crack at the end of the starter bars with this crack reaching a width of 1.5 mm at the completion of this cycle. The subsequent load reversal resulted in cracking at the base of the floor-to-beam interface during loading to +0.5% drift. The application of pull-off deformation during the first cycle to -1.0% drift however resulted in the rupturing of the unit-to-beam interface (see Figure 24b) at the end of the unit, with most of height of the interface having ruptured during the previous cycle to +0.5%. It was considered that the application of tension through the unit resulted in a reduced moment demand at the end of the starter bars and, as the objective of this test was to induce a negative moment failure at the end of the starter bars, the test was continued with only rotational deformation applied to the support connection.

During the subsequent negative loading cycles to -2.0% and -3.0%, the drop in capacity of the cracked floor-to-beam interface resulted in most of the applied deformation being concentrated at this location and plastic straining of the starter bars (see Figure 24c). It was not until the loading cycle to -4.5%, at which point the starter bars were close to reaching their ultimate capacity, that the demand at the end of the starter bars was sufficient to induce inelastic strains in the mesh, resulting in the onset of fracturing of these bars. The subsequent drop in capacity at the end of the starter bars meant that further deformation was solely concentrated at this location and no further strain was sustained by the starter bars at the floor-to-beam interface. Figure 24d shows the state of the floor following the completion of the cycle to -4.5%. Following this this cycle, the negative rotational deformation was increased until the remaining mesh bars fractured, resulting in collapse of the floor as shown in Figure 24e. The mesh bars were measured by gauge 11 (see Figure 8a) to fracture once the crack at the end of the starter bars reached a width of between 3 mm and 5 mm, indicating the non-ductile nature of this failure mode if stronger starter bars or an uncracked section had prevented such significant strains from being sustained at the floor-to-beam interface prior to this negative moment failure.

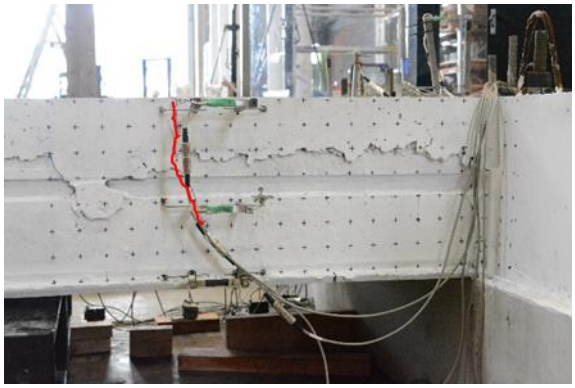

a) -0.5% drift

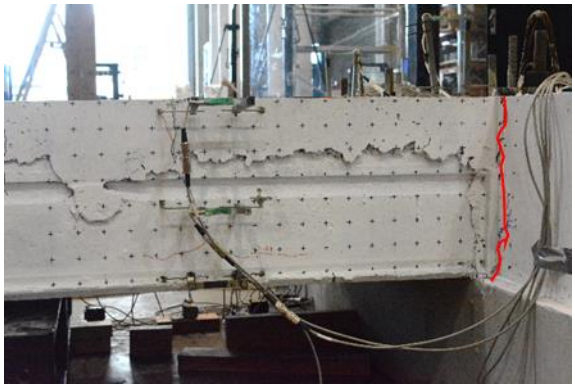

b) -1.0% drift

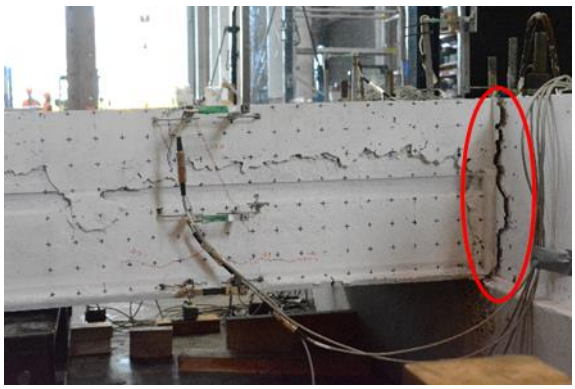

c) -3.0% drift

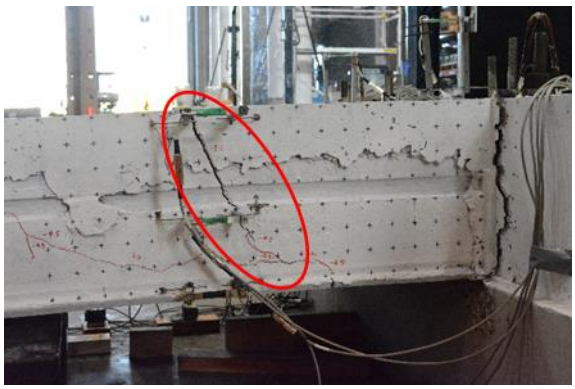

d) -4.5% drift

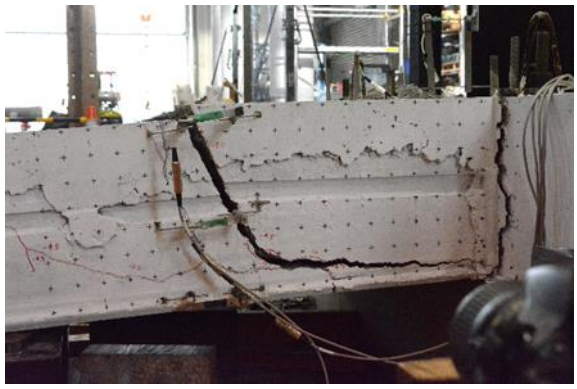

e) Collapse due to negative moment failure

Figure 24. HC4 test progression photos

Measured response

The response of the connection is illustrated in Figure 25a and it can be seen that the moment sustained at the connection during the cycles following cracking at the floor-to-beam interface was less than that which had caused yielding of the mesh during the earlier cycle to -0.5% drift. Approximately the same negative moment demand was induced at a drift of approximately -3.8% as that had been sustained by the uncracked interface at -0.5% drift, causing plastic straining and fracture of the mesh as discussed above. Figure 25b illustrates the bending moment demand along the floor as the maximum negative moment demand was induced and the mesh was yielding. It can be seen that for the mesh to approach ultimate capacity at the location where the starter bars were

terminated, the starter bars must also be very close to ultimate capacity at the floor to beam interface. As discussed above, the bending moment profile in the floor was unrealistically shallow during this test, meaning that for a regular 300HC floor, the starter bars would either have to be stronger or terminate close to the support to induce sufficient demand to induce this failure.

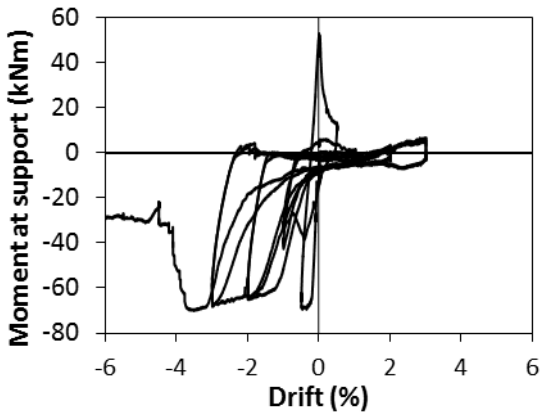

a) Response at support connection

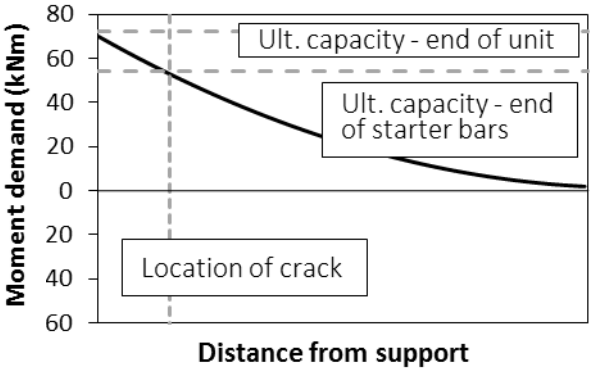

b) Moment demand at maximum negative moment

Figure 25. HC4 moment-rotation response

Figure 26 compares the measured deformations of both the crack in the topping at the floor-to-beam interface as well as the crack at the end of the starter bars. The gauges at each location confirm the observations discussed above and show that the applied deformation was almost solely concentrated at the end of the unit during the cycles to ±1.0%, ±2.0% and ±3.0% drift, following which the demand at the end of the starter bars became sufficient to cause further deformation and ultimately failure of the floor to occur here.

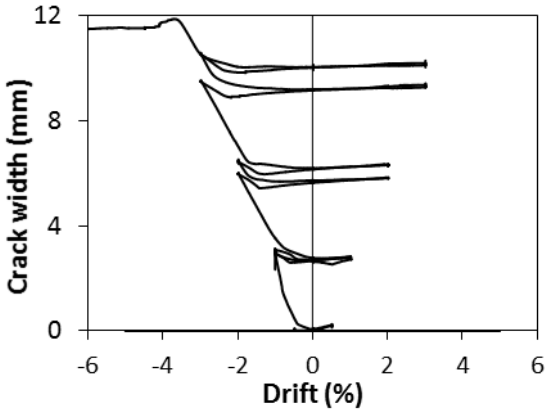

a) Topping crack width at end of unit (gauge 3)

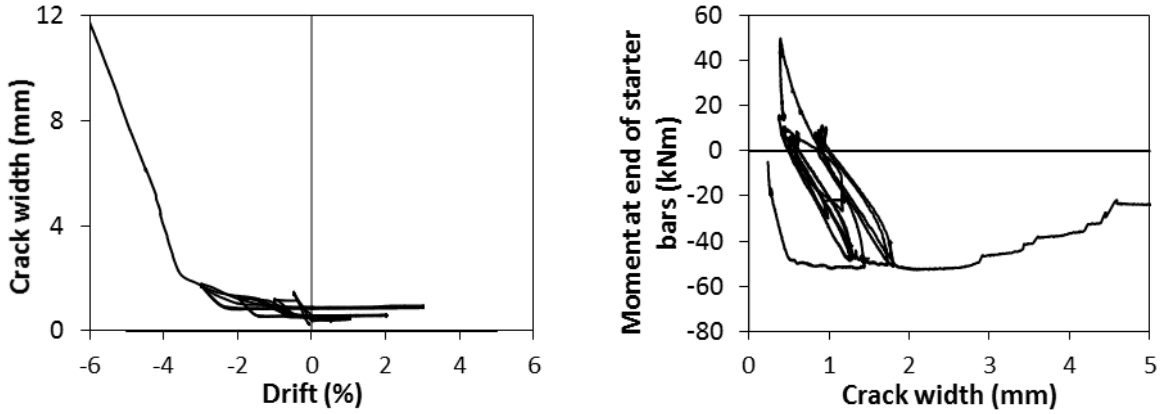

b) Topping crack width at end of starter bars (gauge 11)

Figure 26. HC4 measured deformations

Key results summary

An experimental testing programme has been performed to investigate the residual capacity of hollow-core precast concrete floors containing various damage patterns as observed in Wellington buildings following the 2016 Kaikoura earthquake. By extension, the outcomes of the performed tests have been able to assist in the development of guidelines to assess precast concrete floors and indicate where retrofit of such floors is required. The implications of the results of the four performed tests are discussed below.

Implications to negative moment failure

Negative moment failures were induced during the testing of both specimens HC1 and HC4 while a lack of demand at the end of the starter bars meant that this failure was unable to be induced during the testing of specimen HC3. The key outcome of these two tests was in determining the combination of support connection detailing and loading demands required to induce this failure as well as the deformation capacity of this failure mode once initiated. Where this failure mode was initiated, it was found that fracture of the mesh and failure of the floor would ensue at a crack width of approximately 5 mm at the critical section. During the testing of specimen HC1, damage sustained sufficiently close to the support as well as a lack of presence of starter bars in the floor meant that the negative moment failure was enabled to develop. During the testing of specimen HC4, the use of starter bars of moderate strength and length as continuity reinforcement meant that an unrealistically low gravity demand was required to induce the negative moment failure to occur. Additionally, during both of these tests it was required for the section to be precracked for the negative moment failure to be induced due to the fact that the cracking capacity of the concrete was higher than the ultimate capacity of the floor. As such the following situations result in a floor being more susceptible to a negative moment failure:

- Strong starter bars.
- Starter bars terminating close to the support.
- Low gravity loads.

Implications to positive moment failure

It was attempted during the testing of both specimens HC2 and HC3 for a positive moment crack to be induced approximately 300 mm from the support. However, despite the attempts made to induce this crack in a laboratory environment, the targeted damage was unable to be achieved in either specimen due to the magnitude of the cracking capacity of the unit where the prestressing strands are significantly developed. As a result of the inability to induce this crack, the question has been raised as to how these cracks could have occurred in hollow-core units within existing buildings. The authors consider it to either be the result of the stresses imposed on a unit shortly after casting or the retraction of the prestressing strands following release which would reduce the level of stress in the strands and therefore the contribution of the strands to the cracking capacity of the section.

Both specimens HC1 and HC2 failed as a result of the magnitude of the positive moment crack width close to the support connection and, as such, are able to provide insight into the limit of this crack width for shear to still able to be transferred to the support. During both of these tests, it was deemed that floor reliable load paths in the floor had been lost once the width of this crack was approximately 0.5 times the strand diameter while collapse of the floor was ultimately brought about at a crack width of approximately 1.5 strand diameters.

Implications to loss of support failure

A loss of support failure was investigated during the testing of specimen HC3. The primary outcome of this test was to assist in the development of precast concrete floor assessment procedures by providing a probable combined spalling length of the support beam ledge and end of the unit during a loss of support failure. The point at which significant vertical dislocation of the floor was initiated indicated that the spalling length was 33 mm at a maximum sustained drift of 2.0%.

Acknowledgements

The authors would like to acknowledge the Natural Hazards Research Platform for the financial support provided to this project. The authors would also like to acknowledge the contribution provided to this research project by Dr. Reza Hassanli from the University of South Australia as well as the work performed on the project by ME student Hogan Luo and undergraduate students Frank Büker, Brandon Hill and Tony Wang.

References

Brunsdon, D., Hare, J., and Elwood, K. (2017). "Engineering assessment processes for Wellington buildings following the November 2016 Kaikoura earthquakes". *Bulletin of the New Zealand Society for Earthquake Engineering*, 50(2), 338-342.

Corney, S. R., Henry, R. S., and Ingham, J. M. (2014). "Performance of precast concrete floor systems during the 2010/2011 Canterbury earthquake series". *Magazine of Concrete Research*, 66(11), 563-575.

Fenwick, R., Bull, D., and Gardiner, D. (2010). *Assessment of hollow-core floors for seismic performance* (2010-2). Christchurch, New Zealand: Dept. of Civil and Natural Resources Engineering, University of Canterbury. Retrieved from http://www.ir.canterbury.ac.nz/bitstream/handle/10092/4211/12626196_CNRE%20Assessment%20of%20Hollow-core%20Floors%20for%20Seismic%20Performance.pdf?sequence=1

Henry, R. S., Dizhur, D., Elwood, K. J., Hare, J., and Brunsdon, D. (2017). "Damage to concrete buildings with precast floors during the 2016 kaikoura earthquake". *Bulletin of the New Zealand Society for Earthquake Engineering,* 50(2), 174-186.

Iverson, J., and Hawkins, N. (1994). "Performance of precast/prestressed concrete building structures during Northridge earthquake". *Precast concrete institute (PCI) journal special report,* 39(2), 38-55.

Jensen, J. (2006). *The seismic behaviour of existing hollowcore seating connections pre and post retrofit.* ME thesis, Dept. of Civil Engineering, University of Canterbury, Christchurch, New Zealand.

Kestrel Group. (2017). *Wellington City Council Targeted Assessment Programme Following the Kaikoura Earthquake of 14 November 2016.* Wellington, New Zealand.

MacPherson, C. (2005). *Seismic performance and forensic analysis of precast concrete hollow-core floor super-assemblage.* ME thesis, Dept. of Civil Engineering, University of Canterbury, Christchurch, New Zealand.

Matthews, J. (2004). *Hollow-core floor slab performance following a severe earthquake.* PhD thesis, Dept. of Civil Engineering, University of Canterbury, Christchurch, New Zealand.

Park, R. (2002). "Seismic design and construction of precast concrete buildings in New Zealand". *PCI Journal,* 60(2), 60-75.

Standards New Zealand. (2002). Structural Design Actions Part 0: General principles, NZS 1170.0 2002. Wellington, New Zealand.

Standards New Zealand. (2006). Concrete Structures Standard, NZS 3101 2006, including amendments 1 and 2 (2008). Wellington, New Zealand.

Woods, L. (2008). *The significance of negative bending moments in the seismic performance of hollow-core flooring.* ME thesis, Dept. of Civil Engineering, University of Canterbury, Christchurch, New Zealand.